ELSEVIER

NeuroImage

www.elsevier.com/locate/ynimg
NeuroImage xx (2006) xxx – xxx

Somatosensory cortical plasticity in carpal tunnel syndrome—A cross-sectional fMRI evaluation

Vitaly Napadow,[a,b,*] Norman Kettner,[b] Angela Ryan,[c] Kenneth K. Kwong,[a] Joseph Audette,[c] and Kathleen K.S. Hui[a]

[a]*Martinos Center for Biomedical Imaging, Department of Radiology, Massachusetts General Hospital, Charlestown, MA, USA*
[b]*Department of Radiology, Logan College of Chiropractic, Chesterfield, MO, USA*
[c]*Spaulding Rehabilitation Hospital, Boston, MA, USA*

Received 11 September 2005; revised 9 November 2005; accepted 15 December 2005

Carpal tunnel syndrome (CTS) is a common entrapment neuropathy of the median nerve characterized by paresthesias and pain in the first, second, and third digits. We hypothesize that aberrant afferent input in CTS will lead to cortical plasticity. Functional MRI (fMRI) and neurophysiological testing were performed on CTS patients and healthy adults. Median nerve innervated digit 2 (D2), and digit 3 (D3) and ulnar nerve innervated digit 5 (D5) were stimulated during fMRI. Surface-based and ROI-based analyses consistently demonstrated more extensive and stronger contralateral sensorimotor cortical representations of D2 and D3 for CTS patients as compared to healthy adults ($P < 0.05$). Differences were less profound for D5. Moreover, D3 fMRI activation in both the contralateral SI and motor cortex correlated positively with the D3 sensory conduction latency. Analysis of somatotopy suggested that contralateral SI representations for D2 and D3 were less separated for CTS patients (3.8 ± 1.0 mm) than for healthy adults (7.5 ± 1.2 mm). Furthermore, the D3/D2 separation distance correlated negatively with D2 sensory conduction latency—the greater the latency, the closer the D2/D3 cortical representations ($r = -0.79$, $P < 0.05$). Coupled with a greater extent of SI representation for these CTS affected digits, the closer cortical representations can be interpreted as a blurred somatotopic arrangement for CTS affected digits. These findings provide further evidence that CTS is not manifest in the periphery alone. Our results are consistent with Hebbian plasticity mechanisms, as our cohort of CTS patients had predominant paresthesias, which produce more temporally coherent afferent signaling from affected digits.

Keywords: Somatotopy; Nerve entrapment; Neuropathy; Hebbian plasticity; Disinhibition

Carpal tunnel syndrome (CTS) is the most common entrapment neuropathy. A recent cross-sectional study revealed a prevalence in the United States of 3.72% (Papanicolaou et al., 2001). CTS etiology is characterized by compression of the distal median nerve by an elevated pressure in the carpal tunnel. Ischemic injury to the median nerve induces a range of symptoms primarily in the first through fourth digit, including paresthesias, pain, and weakness. Paresthesias represent the most common symptom (Nora et al., 2005) and result from ectopic impulse activity generated by ischemic nerve damage (Ochoa and Torebjork, 1980; Mogyoros et al., 2000).

In CTS, median nerve injury leads to altered afferent processing throughout the somatosensory system (e.g., peripheral and central nervous systems), as measured in the spinal cord, brainstem, and primary sensorimotor cortex (SMC) by somatosensory evoked potentials (Tinazzi et al., 1998). CTS manifestations in the contralateral SMC have also been studied by magnetoencephalography (MEG). A case study report suggested that the primary sensory representation of ulnar nerve innervated digit 5 (D5) may shift laterally into median nerve innervated digit territory (Druschky et al., 2000). Another MEG study of CTS found that the digit 1 (D1) to D5 cortical representation distance depended on the patients' qualitative symptomatology—expansion when paresthesias prevailed and contraction when pain prevailed (Tecchio et al., 2002). Furthermore, this study found an amplified response for median nerve innervated digit 3 (D3) as compared to ulnar nerve innervated D5, and interpreted this result as cortical amplification of a reduced amount of specific tactile information from affected digits.

The digits occupy a significant portion of the somatotopic map in the primary somatosensory cortex and are represented in consecutive order along the post-central gyrus, with D1 most ventrolateral and D5 most dorsomedial (Penfield and Boldrey, 1937). Cortical plasticity in digit somatotopy has been investigated following experimentally induced decreased, increased, and aberrant afferent signaling. Decreased afferent input has been induced by digit amputation or median nerve section, producing invasion of deafferentated primary sensory cortical fields by adjacent fields from intact digits (Merzenich et al., 1983, 1984). Conversely, electro-

* Corresponding author. 149 13th St. Rm. 2301, Charlestown, MA 02119, USA. Fax: +1 617 726 7422.
E-mail address: vitaly@nmr.mgh.harvard.edu (V. Napadow).
Available online on ScienceDirect (www.sciencedirect.com).

1053-8119/$ - see front matter © 2005 Elsevier Inc. All rights reserved.
doi:10.1016/j.neuroimage.2005.12.017

physiology and fMRI studies have shown that increased afferentation by tactile stimuli enlarges the SI cortical receptive field (Jenkins et al., 1990; Hodzic et al., 2004). Electrophysiology studies of atypical afferent signaling have demonstrated that surgically fusing adjacent digits produces blurred cortical representations of the affected digits (Allard et al., 1991). A similar result is also obtained by training a monkey with temporally coherent multi-digit stimulation (Wang et al., 1995).

As CTS is characterized by dysesthesias, or unpleasant atypical sensations, and pain, we hypothesize that this aberrant afferent input will lead to cortical plasticity. While previous studies of CTS-induced cortical plasticity have utilized MEG, CTS has never been studied with fMRI. This imaging modality has improved spatial resolution, whole brain coverage, and can provide important complementary information. For example, the extent of cortical field representations for individual digits cannot be detected by somatosensory evoked field amplitudes or equivalent current dipole moments. fMRI has been used to non-invasively map digit somatotopy (Gelnar et al., 1998; Kurth et al., 1998; McGlone et al., 2002), and we have adopted this modality to study central reorganization associated with CTS.

Methods

This cross-sectional study was completed in conjunction with a pilot clinical trial of acupuncture for the treatment of CTS, though the data used in this study were taken before any treatment had occurred. All participants in the study provided written informed consent in accordance with the Human Research Committee of the Massachusetts General Hospital.

Subject recruitment and evaluation

A total of 25 subjects were enrolled in this study; 13 adults affected by CTS, and 12 healthy adults. Clinical evaluation was completed for both groups by an experienced physician [JA] at the Spaulding Rehabilitation Hospital, and included medical history, nerve conduction studies (Cadwell Sierra EMG/NCS Device, Kennewick, WA), grip strength (BTE Work Simulator, Hanover, MD), sensory threshold testing using Semmes Weinstein monofilaments, and testing for Phalen's and Tinel's sign. Nerve conduction studies (NCS) using the method described by Ma and Liveson (1983) were performed with stimulation at the 2nd wrist crease on both the median and ulnar nerves of the most symptomatic hand (based on subject history). Both groups also completed the Boston Carpal Tunnel Syndrome Questionnaire (Levine et al., 1993). Subjects were screened and excluded for psychiatric and neurological disorders, head trauma with loss of consciousness, or other serious cardiovascular, respiratory or renal illness. CTS patients were included if they had experienced pain and/or paresthesias for greater than 3 months in the median nerve distribution of the affected hand—D1, D2, D3, and the radial aspect of D4. Furthermore, NCS findings needed to be consistent with mild to moderate CTS. Mild CTS was defined by delayed distal latency of median sensory nerve conduction across the wrist (>3.7 ms and/or >0.5 ms compared to ulnar sensory nerve conduction) with normal motor nerve conduction (Stevens, 1997; You et al., 1999). Moderate CTS was defined by mild CTS and with delayed distal latency of median motor nerve conduction across the wrist (>4.2 ms), but with normal motor amplitudes. Patients with severe CTS, defined by prolonged median sensory and motor latencies with either absent sensory nerve action potentials and/or reduced (50%) median motor amplitudes, were excluded. Patients were also excluded if they demonstrated any sign of generalized peripheral neuropathy or localized ulnar nerve entrapment.

fMRI data analysis was completed on a total of 10 CTS patients (6 female, 4 male; mean age: 51.1, range 31–60) and 9 age and gender-matched healthy adults (6 female, 3 male; mean age: 46.9, range 32–59). Of the 13 CTS patients initially studied, one was removed for excessive motion during fMRI scanning, and two were removed because they dropped out of the study immediately after the initial clinical and fMRI evaluation and did not complete adequate structural scans for surface reconstruction. Of the 12 healthy adults initially studied, one subject was removed from the fMRI analysis due to excessive motion artifact, one for lack of somatosensory response, and one for an acute finger injury (unrelated to the study). Five patients presented with CTS symptoms in both hands, while 5 presented with only unilateral symptomatology. For patients with bilateral CTS, testing was done on the more affected hand (self report). In all cases, the more affected hand was also the patient's dominant hand. The chronicity of symptoms (self reported) ranged from 4 months to 10 years, with 8 of 10 patients having symptoms for longer than 1 year. While patients reported both pain and paresthesias, a pain/paresthesia ratio was calculated from subjective responses to individual questions of the BCTSQ (pain: Q1–Q5, paresthesia: Q6–Q10).

fMRI image acquisition and stimulation protocol

Functional scans were acquired using a 3.0 T Siemens Allegra MRI System equipped for echo planar imaging with quadrature head coil. The subject lay supine in the scanner with the head immobilized using a cushioned support.

Two sets of structural images were collected using a T1-weighted MPRAGE sequence (TR/TE = 2.73/3.19 ms, flip angle = 7°, FOV = 256 × 256 mm; slice thickness = 1.33 mm). Blood oxygenation level-dependent (BOLD) functional imaging was performed using a gradient echo T2*-weighted pulse sequence (TR/TE = 3000/30 ms, flip angle = 90°, FOV = 200 × 200 mm, 38 sagittal slices, slice thickness = 3.0 mm with 0.6 mm interslice gap, 90 image volumes per slice, matrix = 64 × 64). Image collection was preceded by 4 dummy scans to allow for equilibration of the MRI signal.

During an fMRI session, three digits were individually stimulated in a pseudo-randomized manner, for 3 scan runs each. Digits were chosen from the more affected hand of CTS patients (right hand: $n = 8$) and on the dominant hand of healthy adult volunteers (right hand: $n = 8$). The stimulated digits included D2, D3, and D5; thereby testing the somatosensory response for affected (*median n.*, D2, D3) and non-affected (*ulnar n.*, D5) digits in CTS patients. A single fMRI scan run consisted of a block design protocol with four 30-s blocks of stimulation (ON-block), alternating with five 30-s blocks of no stimulation (OFF-block). Pad electrodes were attached to the volar aspect (glabrous skin) of the middle and distal phalanx of D2, D3, and D5. The stimulus consisted of 100 Hz constant current electrostimulation (HANS LH202H, Neuroscience Research Center, Peking University, Beijing, China). In order to avoid habituation, the peak amplitude of the 100 Hz electrostimulation was modulated ±25% by a slow varying sinusoidal envelope (0.2 Hz) throughout each 30 s ON-block. The current strength of stimulation during each scan was

chosen to be 0.2 mA below the pain threshold in order to normalize for differences in pain and somatosensory sensitivity, particularly because CTS is reported to involve abnormal somatosensory threshold levels (Nishimura et al., 2003). Current level was tested immediately prior to each scan to assure that the stimulus was not painful. Subjects were instructed to keep their eyes closed, and to pay close attention to the sensations felt at the stimulated digit.

Single subject fMRI data analysis

Analysis was carried out using a combination of software including FEAT (fMRI Expert Analysis Tool) Version 5.1, part of FSL (FMRIB's Software Library, www.fmrib.ox.ac.uk/fsl), surface mapping (SUMA) in AFNI (Cox, 1996), and Freesurfer (Dale et al., 1999). Data collected for left-hand dominant healthy adults (1 subject) or who had predominant left-handed CTS symptoms (2 subjects), were mirror reversed across the mid-sagittal plane. The following pre-statistics processing was applied: motion correction using MCFLIRT (Jenkinson et al., 2002); non-brain removal using Brain Extraction Tool, BET (Smith, 2002); spatial smoothing using a Gaussian kernel of FWHM 5 mm; mean-based intensity normalization; and highpass temporal filtering (sigma = 30.0 s). Time-series statistical analysis was carried out using FILM (FMRIB's Improved Linear Model) with local autocorrelation correction (Woolrich et al., 2001). The hemodynamic response function utilized in the general linear model (GLM) analysis was defined by the block design paradigm convolved with a prescribed gamma function (standard deviation = 3 s, mean lag = 6 s).

Structural T1-weighted MPRAGE images from each subject were averaged, and the Freesurfer software package was used to generate a model of the cortical surface through intensity normalization, skull-stripping, segmentation and tessellation of the gray-white matter interface surface (Dale et al., 1999). This reconstructed cortical surface was inflated using spring force and metric-preserving terms. The tessellated surface was also projected onto a unit sphere (spherical space), using algorithms that minimize metric distortions, thereby parameterizing the surface into a spherical-based coordinate system (Fischl et al., 1999a). The cortical surface of each subject brain was normalized to an average brain template by maximizing alignment of the folding patterns in a spherical representation (Fischl et al., 1999b), a process that provides more accurate group averaged statistical analysis over surface elements from topologically homologous regions in the brains of different subjects. Similar surface-based analyses for somatosensory mapping in SI have been used in the past (Moore et al., 2000). These post-processing techniques improve both anatomical region attribution and functional data visualization by respecting the topological curvature inherent in the sulcal and gyral structure found around the central sulcus. Hence, these techniques are especially suited for studies of somatotopy, as described below.

Surface-based group fMRI data analysis

Functional images from each subject were co-registered with their averaged T1-weighted MPRAGE structural volume using an automated procedure that included manual adjustment with particular focus on central sulcus coregistration. Separate scan runs for each stimulated digit were checked for excessive motion artifact (removed from analysis if >3 mm motion on any axis), and averaged under a fixed effects model. The change in signal intensity from baseline (in %) was then calculated for each digit. The mean percent signal change taken along a normal vector through the cortical gray matter thickness was calculated and normalized to a standard mesh surface. Group maps for each stimulated digit and activation difference maps (CTS patients versus healthy adults) were calculated using a fixed effects statistical model, thus results cannot be extrapolated to the population. Resultant statistical parametric maps were corrected for multiple comparisons at a false discovery rate (FDR) of 0.05 (Genovese et al., 2002) and clustered at an area equivalent to the cross-section of 3 image voxels (29.3 mm^2). To investigate any temporal differences in somatosensory response, we also analyzed the fMRI time course from the node of greatest percent signal change in Brodmann Area 1 (BA1, see ROI analysis below). Time courses were de-trended and smoothed. The peak fMRI response during successive ON blocks was compared between CTS patients and healthy adults with an unpaired Student's t test.

ROI-based fMRI data analysis

The extent of SMC activation and somatotopy were quantified with the aid of user defined anatomical ROIs, outlined on the smoothed white matter (gray/white boundary) surface (SUMA, AFNI; Fig. 1). The ROIs were putative BA1, defined as the crest of the postcentral gyrus, and putative BA4, defined as the anterior bank of the central sulcus (Gelnar et al., 1998; Moore et al., 2000). The "putative" qualification is due to inexact correspondence between cytoarchitectonic and topological border definitions (Rademacher et al., 1993; White et al., 1997). The superior margin of the ROIs was taken to be the superior edge of the hemisphere, thereby avoiding potential contamination from dorsal inter-hemispheric vein artifacts. The inferior edge of the ROIs was defined by a posterior extension of the inferior frontal sulcus, thereby avoiding the parietal operculum. BA1 was chosen over BA3b because primary somatosensory cortex activation in response to our stimulus could be localized in BA1 for every subject and patient, whereas BA3b activation was less common under our threshold and cluster criteria (healthy adults: 9/9 D2, 7/9 D3, 6/9 D5; CTS patients: 8/10 D2, 9/10 D3, 8/10 D5). Somatotopy in BA1 has been reported by imaging studies (Blankenburg et al., 2003; Overduin and Servos, 2004), while electrophysiological studies have also noted a crude and overlapping, but still topologically consistent finger representation in monkeys (Kaas et al., 1979; Iwamura et al., 1985). In addition, other fMRI investigations have also found BA1 activation to be more universal than BA3b (Gelnar et al., 1998; McGlone et al., 2002). Gelnar at al. attributed the greater universality of BA1 activation to high stimulus frequency (50 Hz vibrotactile), which may have also explained the results of McGlone et al., who used 80 Hz vibrotactile stimulation in their study, as well as our results with 100 Hz electrostimulation. This frequency dependent response may be due to the fact that BA1 neurons respond more readily to stimuli from rapidly adapting receptors (Kaas et al., 1979). BA4 was investigated due to previously noted cutaneous anatomical inputs to the precentral gyrus (Strick and Preston, 1978; Wong et al., 1978). In addition, precentral gyrus activation has been noted by other fMRI studies with tactile somatosensory (Francis et al., 2000; McGlone et al., 2002) and even proprioceptive stimuli (Mima et al., 1999; Naito et al., 2002). Furthermore, we wanted to explore if this region was affected in CTS as precentral gyrus disinhibition

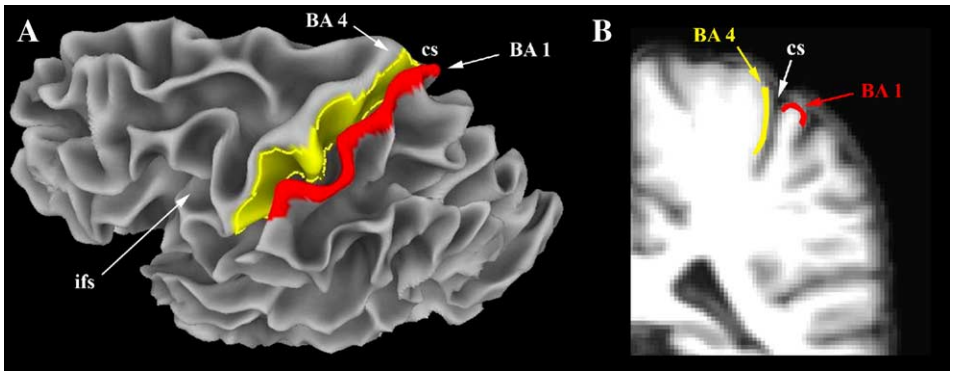

Fig. 1. Regions of interest (ROIs) were defined on the contralateral hemisphere for each individual. (A) Putative BA1 was defined as the crest of the postcentral gyrus, while putative BA4 was defined as the anterior bank of the precentral gyrus. The lateral extent of the ROIs was defined by the posterior extension of the inferior frontal sulcus (ifs). The central sulcus is labeled (cs) on the smoothed white matter/gray matter boundary surface above. (B) BA1 and BA4 ROI's are visualized in a coronal cross-section.

has been reported for other chronic pain states (Juottonen et al., 2002; Schwenkreis et al., 2003; Eisenberg et al., 2005). The extent of activation for each individual was defined as the surface area of statistically significant fMRI signal increase. The mean extent of activation in BA1 and BA4 ROIs was compared between CTS patients and healthy adults with an unpaired Student's t test (significant for $\alpha < 0.05$).

Somatotopy was assessed in each individual by localizing the percent signal change center-of-mass of the largest hand area cluster in BA1, contralateral to digit stimulation (Fig. 1). The hand area in SI was defined broadly as the postcentral gyrus involution adjacent to the omega shaped fold in the central sulcus around a knob in the precentral gyrus (Yousry et al., 1997). The center-of-mass location for each digit tested in each individual was projected to the group-averaged surface (standard mesh) to assure inter-group comparability. The location was defined on the group-averaged surface by the surface-based distance from a common convenient landmark—the lateral edge of the parietal operculum on the crest of the post-central gyrus. Center-of-mass digit representations in BA1 and D2/D3 separation distance were compared between CTS patients and healthy adults with an unpaired Student's t test (significant for $P < 0.05$). Through increased sensitivity due to inter-subject averaging and center-of-mass calculations, spatial differences in somatotopy between patients and controls could be derived that approached the single subject voxel resolution and smoothing kernel bandwidth.

Results

Neurophysiological results

In our cohort of patients, paresthesias were more dominant than pain in 7/10 patients, as derived from self-report in the BCTSQ. The remaining 3/10 patients had pain/paresthesia ratios between 1.0 and 1.1 (i.e., close to an equal amount of pain and paresthesias). In sum, CTS patients reported a pain/paresthesia ratio of 0.74 ± 0.08 (μ ± SEM). In our cohort of CTS patients, the average median nerve sensory latency for D2 and D3 was 3.48 ± 0.05 ms (μ ± SEM) and 3.80 ± 0.07 ms, respectively, compared to an ulnar nerve sensory latency for D5 of 2.12 ± 0.04 ms. CTS patients also had an average median motor distal latency of 4.58 ± 0.09 ms. In contrast, healthy adults had an average sensory latency for D2 and D3 of 2.40 ± 0.02 ms and 2.39 ± 0.03 ms, respectively, compared to ulnar sensory latency for 2.13 ± 0.02 ms. Healthy adults also had an average median motor distal latency of 3.44 ± 0.07 ms.

fMRI surface-based group comparisons

Innocuous electrostimulation applied to D2, D3, and D5 produced activation in similar brain regions for both healthy adults and CTS patients (Fig. 2, Table 1). fMRI signal increase was seen in the contralateral pre-central and post-central gyrus (motor cortex and SI, respectively). Activity was also seen in both the contralateral and ipsilateral parietal operculum, consistent with secondary somatosensory area (SII) and ventral parietal area (PV), as well as rostral and caudal regions in the upper bank of the Sylvian fissure adjacent to SII/PV. Activation was also noted in the posterior parietal fields (sensory association cortex, BA5/7 and BA40), the contralateral thalamus, and the ipsilateral cerebellum (not shown). Activation was observed less consistently in the insula, as well as prefrontal cortical and superior temporal regions for both groups. While these global findings were seen in both CTS patients and healthy adults, the extent and localization of activation in the SMC demonstrated that significant differences did exist between the two groups.

The group activation maps for median nerve innervated D2 and D3 demonstrated greater extent of activation in the contralateral pre-central and post-central gyrus for CTS patients as compared to healthy adults (group maps, Fig. 2; statistical difference maps, Fig. 3). In contrast to the ipsilateral sensorimotor signal decreases for healthy adults, the ipsilateral SMC for CTS patients demonstrated less profound signal decrease (D3), or no decrease at all (D2). Results for ulnar nerve innervated D5 between CTS patients and healthy adults appeared more similar, although CTS patients did show greater response in the pre-central gyrus (Fig. 3). There was not a significant difference in the ipsilateral hand primary sensorimotor area between the two groups for D5. Time course analysis of activation in contralateral SI showed that the peak percent signal change was greater for CTS patients than for healthy adults (Fig. 2). Specifically, for D2, the difference in peak amplitude for individual ON-blocks was 0.28 ± 0.08 (μ ± σ, unpaired t test, $P < 0.005$). For D3, the difference was 0.19 ± 0.03 ($P < 0.001$). There was no significant difference for D5: −0.02 ± 0.08 ($P > 0.1$). Neither group demonstrated

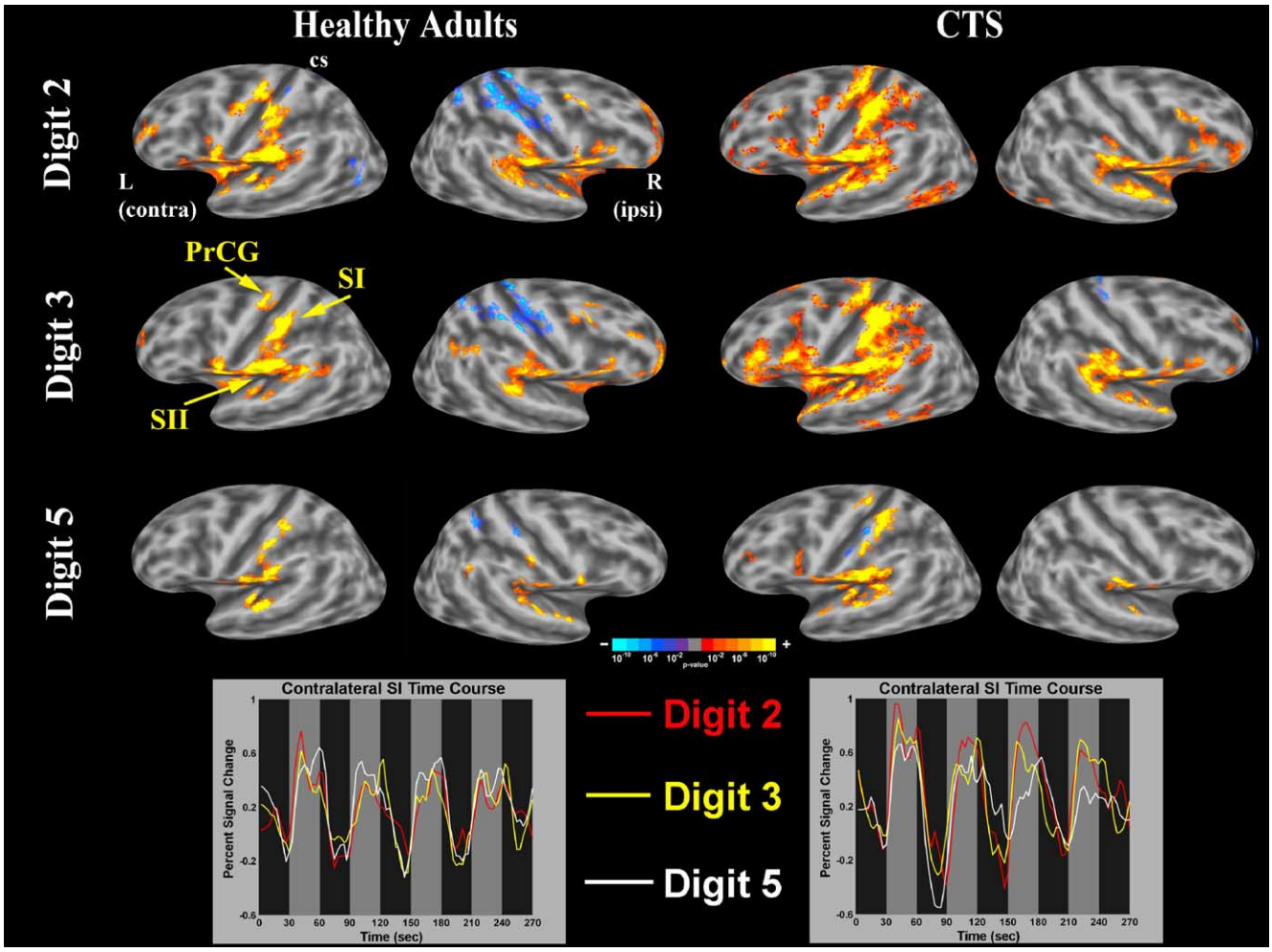

Fig. 2. Group maps for CTS patients and healthy adults for D2, D3, and D5. Activation (color-coded *P* value) was overlaid onto group-averaged inflated brains with grey-scale defined curvature (sulci dark, gyri light). Both right (ipsilateral) and left (contralateral) hemispheres are shown. CTS patients demonstrated more extensive activation than healthy adults in contralateral S1 and motor cortex for median nerve innervated D2 and D3. CTS patients also demonstrated less statistically significant deactivation in ipsilateral SMC for D2 and D3. Differences for ulnar nerve innervated D5 were less profound. fMRI signal time courses demonstrated greater signal increase in all 4 ON blocks for CTS patients compared to healthy adults for D2 and D3, while no significant difference was found for D5 (cs: central sulcus).

statistically significant change in peak fMRI signal for successive ON blocks.

fMRI ROI-based comparisons

An ROI analysis (Fig. 4a) showed that the extent of activation (surface area) in contralateral BA1 with D2 stimulation was greater for CTS patients compared to healthy adults (CTS $\mu \pm$ SEM: 144.6 ± 29.0 mm^2; Healthy: 66.8 ± 15.0 mm^2, $P < 0.05$). Contralateral BA1 activation due to D3 stimulation was also significantly greater for CTS patients as compared to healthy adults (CTS: 162.5 ± 32.2 mm^2; Healthy: 85.4 ± 22.2 mm^2, $P < 0.05$). Contralateral BA1 activation during ulnar nerve innervated D5 stimulation showed a trend for greater activation for CTS patients as compared to healthy adults (CTS: 88.7 ± 33.2 mm^2; Healthy: 53.6 ± 12.7 mm^2, $P = 0.144$).

The findings for contralateral BA4 were similar to the results for BA1 (Fig. 4B), though activation in BA4 was less universal than activation in BA1 for individuals in either group. Activity due to D2 stimulation in contralateral BA4 showed a trend for more extensive activation by CTS patients compared to healthy adults (CTS: 115.3 ± 38.4 mm^2; Healthy: 45.7 ± 13.5 mm^2, $P = 0.053$), while for D3, increased activity in this ROI for CTS patients did reach statistical significance (CTS: 144.7 ± 45.35 mm^2; Healthy: 46.8 ± 21.9 mm^2, $P < 0.05$). Stimulation of D5 showed more activation in contralateral BA4 for CTS patients compared to healthy adults (CTS: 66.3 ± 26.3 mm^2; Healthy: 6.8 ± 3.9 mm^2, $P < 0.05$), though it should be noted that the latter group had only three of nine subjects with any activity in this ROI.

Analysis of somatotopy in contralateral BA1 demonstrated that there was a medial shift of D2 representation by an average 2.7 mm (unpaired Students' *t* test, $P < 0.05$). The mean activation for D2 stimulation was located 36.5 ± 0.9 mm ($\mu \pm$ SEM) dorsal to the lateral edge of the parietal operculum for CTS patients, while D2 activation was only 33.8 ± 1.0 mm from the same reference point for healthy adults (Fig. 5A). However, there was no significant difference in D3 or D5 representation between CTS patients and healthy adults (CTS: D3: 39.1 ± 1.2 mm D5: 44.2 ± 1.4 mm; Healthy: D3: 38.1 ± 1.6 mm D5: 43.2 ± 1.2 mm). Taken together, there was a significant

Table 1
Summary of group map sensorimotor cortical activations with cluster center-of-mass (COM) Talairach coordinates, significance and extent for SI, precentral gyrus, and SII

Group	Digit	Region	Talairach Coordinates			p–value (10^{-x})	Cluster Size (mm^2)
			X (mm)	Y (mm)	Z (mm)		
CTS	2	SI	–51	–15	50	8.40	322.95
		PrCG	–41	–15	58	7.21	166.22
		SII	–51	–12	22	8.75	550.02
	3	SI	–50	–16	52	8.83	520.59
		PrCG	–39	–17	62	6.88	140.08
		SII	–52	–13	22	9.39	702.72
	5	SI	–45	–20	54	7.94	146.57
		PrCG	–39	–19	62	7.55	28.03
		SII	–50	–13	22	8.62	411.17
Norm	2	SI	–47	–15	46	8.73	98.78
		PrCG	–39	–12	54	7.17	126.54
		SII	–52	–13	22	10.05	474.95
	3	SI	–51	–17	51	8.44	175.97
		PrCG	–38	–10	58	6.71	38.54
		SII	–54	–12	22	10.15	330.45
	5	SI	–50	–20	53	6.43	53.65
		PrCG	–	–	–	–	–
		SII	–55	–13	21	7.36	224.12

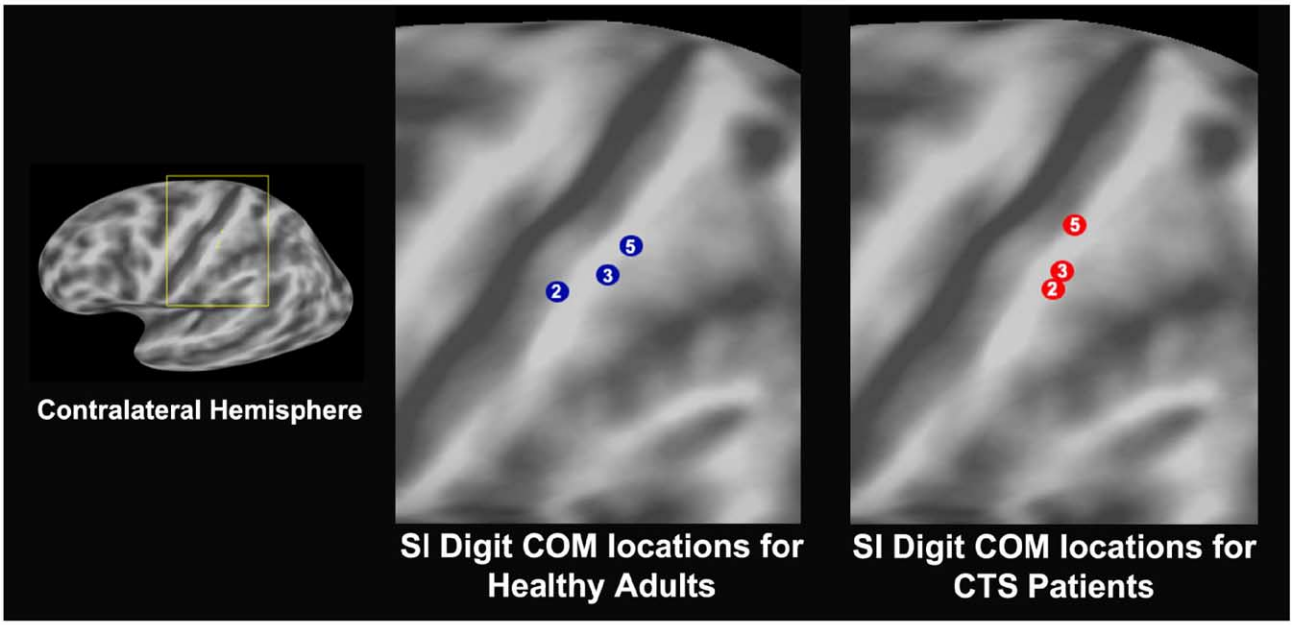

SI COM locations for D2, D3, and D5 are visualized on the inflated surface. The D2 and D3 SI representations were larger and closer together for CTS patients than for healthy adults. (SI: primary somatosensory cortex; PrCG: precentral gyrus; SII: secondary somatosensory cortex; *P* value: mean *P* value for cluster, expressed as 10^{-x}; Cluster Size: size of cluster on the surface, expressed as mm^2).

contraction of the D3/D2 separation distance for CTS patients as compared to healthy adults (CTS: 3.8 ± 1.0 mm; Healthy: 7.5 ± 1.2 mm, $P < 0.05$) (Fig. 5B). Contraction of the D3/D2 separation distance for CTS patients was also clearly demonstrated by visualizing the center-of-mass locations from the group maps (Table 1).

Correlation of fMRI data with neurophysiological assessment

A range of median sensory nerve conduction latencies was found for CTS patients (see above). The conduction latency for D2 was negatively correlated with the D3/D2 separation distance ($r^2 = 0.62$, $P < 0.05$)—i.e., the greater the conduction latency, the closer the distance between D2 and D3 (Fig. 6). No significant correlations were found between the D3/D2 separation distance and other clinical measures such as neuropathic pain severity or symptom chronicity.

Comparison of fMRI stimulus requirement

As we set fMRI stimulus current strength relative to subjects' pain threshold, it was important to evaluate whether differences in stimulus strength may have contributed to differences in fMRI

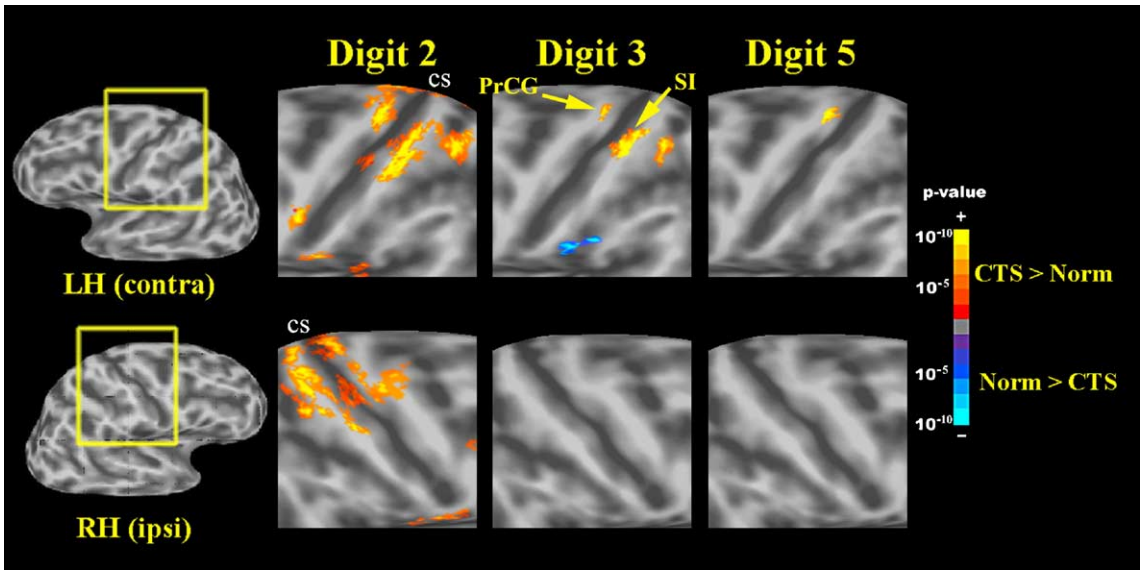

Fig. 3. Difference maps tested the fMRI activation difference between CTS patients and healthy adults for D2, D3 and D5. The contralateral and ipsilateral pre/postcentral gyrus area is shown. Note that red/yellow color-coding refers to either more fMRI signal increase or less fMRI signal decrease for CTS patients as compared to healthy adults. In the contralateral hemisphere, CTS patients demonstrated more extensive activation than healthy adults in S1 for D2 and D3 and in the pre-central gyrus for all three digits. In the ipsilateral hemisphere, CTS patients demonstrated less statistically significant deactivation in the sensorimotor cortex for D2.

results. Though the stimulation intensity varied for different individuals, no significant group differences between CTS patients (digit2 = 6.4 ± 0.6 mA, digit3 = 6.4 ± 0.6 mA, digit5 = 5.1 ± 0.5 mA) and healthy adults (digit2 = 6.0 ± 0.6 mA, digit3 = 5.9 ± 0.6 mA, digit5 = 4.6 ± 0.8 mA) were found for any digit tested. This result suggests better comparability of fMRI findings than if perception matching had led to significantly different group current levels. For both groups, D5 was more sensitive and required significantly less

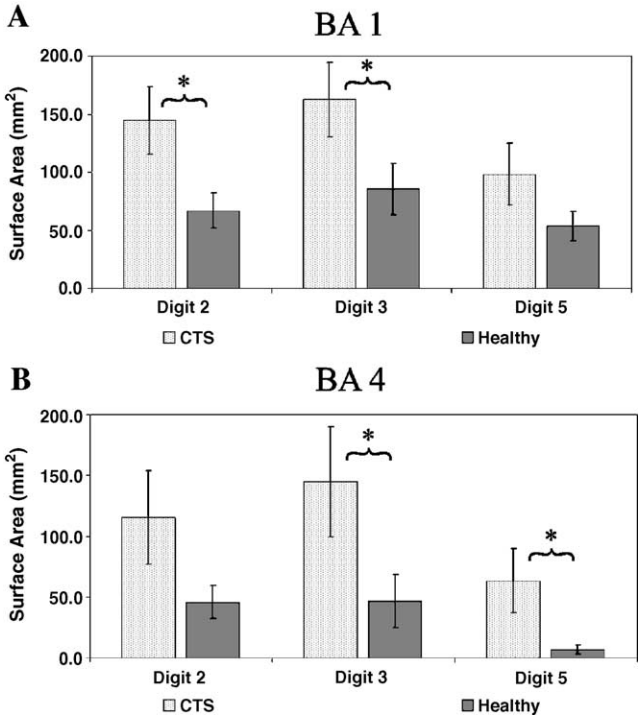

Fig. 4. An ROI analysis on the fMRI data was completed for (A) BA1 and (B) BA4. For BA1, a significantly greater surface area of fMRI activation (*P < 0.05) for CTS patients was found for D2 and D3. For BA4, a significantly greater surface area for CTS patients was found for D3 and D5, though a trend was found for D2 as well (P = 0.053).

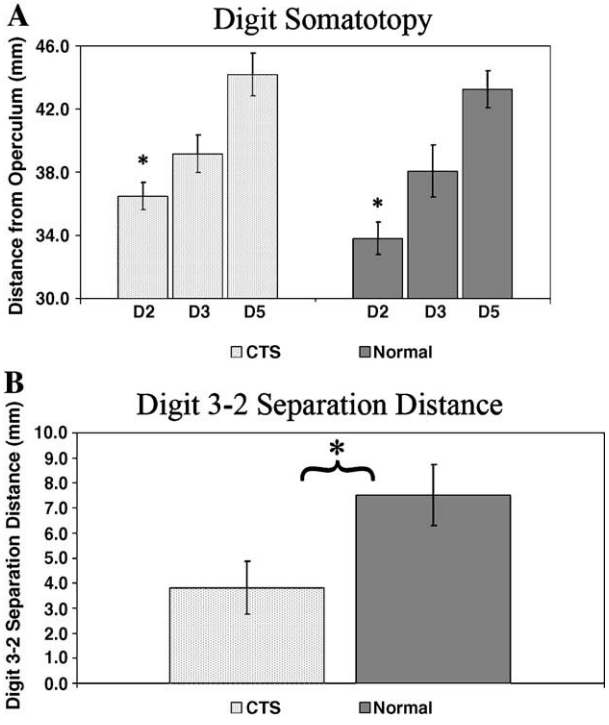

Fig. 5. (A) Somatotopy for CTS patients and healthy adults was defined by the distance of fMRI center-of-mass activation from the lateral edge of the parietal operculum. D2 was found to be shifted medially for CTS patients compared to healthy adults (P < 0.05). (B) This resulted in a decreased D3/D2 separation distance (*P < 0.05), i.e., more blurred representation.

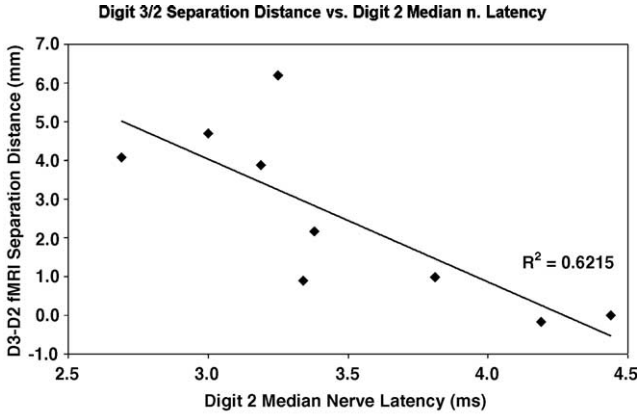

Fig. 6. Correlation analysis demonstrated that neurophysiological variables correlate with fMRI signal outcome measures for CTS patients. The conduction latency for D2 was negatively correlated ($r^2 = 0.62$, $P < 0.05$) with the D3/D2 separation distance—i.e., the greater the peripheral nerve dysfunction, the closer the separation between D2 and D3 for that individual.

current than D2 or D3 (Student's t test, $P < 0.05$). A surface-based correlation analysis did not show statistically significant correlation between fMRI activation and stimulus current strength in any sensorimotor region.

Discussion

To our knowledge, this study represents the first exploration of CTS with fMRI. We have demonstrated that CTS leads to more extensive and overlapping representation in contralateral primary somatosensory cortex of median nerve affected digits. CTS provides an excellent opportunity to investigate cortical reorganization induced by clinically relevant aberrant afferentation in humans.

Extent of fMRI activation

Difference maps, ROI analysis, and time course analysis showed consistently more extensive and amplified contralateral sensorimotor cortical representations for digits affected by CTS as compared to healthy adults. This increased activation in the primary somatosensory cortex is consistent with the M30/M20 ratio amplification found by MEG for median nerve innervated digits in CTS (Tecchio et al., 2002).

We postulate that the increased extent of activation in SI may be due to CTS patients' persistent paresthesias and pain, which represent increased afferent input for the affected digits. Similarly, use-dependent enlargement of cortical representation fields in SI has also been shown for more physiological (non-pathological) states. Electrophysiological mapping and fMRI have demonstrated that increased innocuous tactile stimulation produces enlargement of cortical representation fields in monkeys (Jenkins et al., 1990) and in humans (Hodzic et al., 2004), respectively. The short term mechanism for wider cortical representations in physiological states has been attributed to "disinhibition" (Calford and Tweedale, 1988) due to decreased concentration of γ-aminobutyric acid (GABA, an inhibitory neurotransmitter) in the cortex, which serves to release existing "latent" subthreshold thalamocortical and cortico-cortical excitatory inputs from inhibitory control (Jones, 1993; Dykes, 1997; Levy et al., 2002). With time, these short-term changes may be reinforced via synaptic strengthening from voltage gated, *N*-methyl-D-aspartate (NMDA) receptor mediated long term potentiation, or LTP (Brown et al., 1988; Buonomano and Merzenich, 1998). This process applies to temporally correlated synaptic activity and is known as Hebbian plasticity (Hebb, 1949; Rauschecker, 1991). Similar mechanisms in the cortex may also apply for non-physiological states, such as CTS induced paresthesias and pain—a concept proposed in several recent reports (Ji et al., 2003; Rygh et al., 2005). In fact, other chronic pain states such as complex regional pain syndrome, type I (CRPS I) have also been noted to produce greater SI response to somatosensory stimuli in the form of amplified MEG dipole strength (Juottonen et al., 2002; Maihofner et al., 2003). Thus, while our cohort of patients had paresthesias predominant over pain, their experience with pain may have similarly contributed to increased SI activation.

Increase in extent of activation was also seen in the pre-central cortex for ulnar nerve innervated D5, though there was no difference between group time courses in peak percent change. As we excluded polyneuropathy patients, ulnar nerve conduction was not abnormal and the increase in extent seen for contralateral BA4 may be due to the existence of a "permissive state" favoring non-specific disinhibition and plasticity (Dykes, 1997). This broadly defined permissive state may also explain the less pronounced ipsilateral SMC inhibition (i.e., weaker fMRI signal decrease) in CTS patients.

fMRI activation in the precentral gyrus due to our somatosensory task is consistent with other fMRI studies showing precentral gyrus activation with tactile somatosensory (Francis et al., 2000; McGlone et al., 2002) and even proprioceptive stimuli (Mima et al., 1999; Naito et al., 2002), given that our electrical stimulus may have affected proprioceptors in the distal and proximal interphalangeal joints or their afferents. The more medial location compared to SI activation is consistent with both electrophysiological (Woolsey et al., 1979) and neuroimaging (Maldjian et al., 1999) studies. While there was no muscle tissue beneath stimulus electrodes and hence our stimulus would not be expected to produce muscle twitch, we cannot rule out the possibility that motor cortex activation was the result of digit motion. In addition, the greater motor cortex activation in our CTS patients observed with fMRI is consistent with studies of other chronic pain states. For example, transcranial magnetic stimulation (TMS) (Schwenkreis et al., 2003; Eisenberg et al., 2005) and MEG (Juottonen et al., 2002) studies have demonstrated disinhibition in the contralateral motor cortex for CRPS I.

We also noted activation in parietal operculum regions (SII/PV) as well as regions rostral and caudal to classic SII/PV activation. These extended activations were seen for both CTS patients and healthy adults, and have been noted by other investigators as well (Disbrow et al., 2000). Activity in these extended regions most likely corresponds to the rostral lateral region (RL) and BA 7b, respectively, as described by Disbrow et al. RL receives inputs from PV, while 7b receives inputs from SII.

fMRI digit somatotopy

Analysis of cortical representations in the hand area of contralateral BA1 demonstrated that abnormal afferentation in CTS leads to less separation between median nerve innervated D2 and D3, as compared to healthy adults (CTS: 3.8 ± 1.0 mm; Healthy: 7.5 ± 1.2 mm). This difference in separation was due to a medial

shift in D2 for CTS patients, as the D3 position was not significantly different in the two groups. With deafferentation (e.g., digit amputation), adjacent representations may invade the territory of the deafferentated digit (Merzenich et al., 1983, 1984). However, it is not clear if a medial shift in D2 was coincident with a simultaneous shift in D1 and an invasion from adjacent territory (e.g., lip/chin). In addition, the fact that we did not find a significant group difference in absolute D3 localization may be due to the fact that our patient cohort experienced predominant paresthesias and not classical deafferentation or pain alone. However, there exists more individual variability in absolute digit representation than relative digit ordering—D1 more lateral to D5 more medial (Penfield and Boldrey, 1937; McGlone et al., 2002). Hence, we focused our analysis on a relative measure, namely the D3/D2 separation distance. Furthermore, the D3/D2 separation distance was negatively correlated with the D2 sensory conduction latency—i.e., the worse the peripheral nerve dysfunction, the less separation between D2 and D3. This result suggests that a relationship exists between peripheral neurophysiological findings and imaging results in the brain, further validating the belief that CTS includes a central manifestation of peripheral pathology. Coupled with a greater cortical extent for these digit representations (see above), the closer localization of the D2 to D3 center-of-mass can be interpreted as more overlapping or blurred SI representations.

We propose that the changes in somatotopy detailed with fMRI are due to persistent multi-digit paresthesias. In CTS, paresthesias diffusely spread over D1 to D4 characterize afferent impulses with greater temporal coherence than is normally experienced from these anatomically distinct digits. This temporal synchrony would lead to Hebbian mechanisms of synaptic strengthening and cortical reorganization, such that the cortical representation fields of affected digits become blurred.

Similar cortical reorganization has been noted in somatosensory studies involving manipulation of spatiotemporal patterns of afferent input. For example, investigations of syndactyly, or the skin fold fusion of adjacent digits, involve an unnatural state wherein afferent impulses from affected digits are more closely synchronized in time than from normally separated digits. Electrophysiology studies have shown that surgically induced syndactyly in monkeys produces greater overlap in SI cortical representation fields (Clark et al., 1988; Allard et al., 1991). Furthermore, non-surgical manipulations such as multidigit synchronous co-activation, also produces blurred cortical representations in rat (Godde et al., 1996), primate (Wang et al., 1995), and human (Pilz et al., 2004). Independent digits normally transmit afferent signaling more separated in time than the 5- to 20-ms temporal window necessary for synchronicity amplified LTP. The coactivation animal studies above found that digits with synchronous stimulation showed increased multi-digit receptive fields. The human fMRI coactivation study suggested that the cortical representations for affected digits were closer to one another than prior to co-activation, similar to the blurring of D2 and D3 representations we observed with CTS characterized by multi-digit paresthesias.

Chronic pain states may also lead to shifts in the cortical representation of the affected body part, such as the back representation in patients with chronic low back pain (Flor et al., 1997). In MEG studies of CRPS I, the representations of D1 and D5 were closer to one another on the affected hand (Juottonen et al., 2002; Maihofner et al., 2003), with cortical reorganization (expressed as the lip to D1/D5 midpoint relative distance) correlating with extent of hyperalgesia (Maihofner et al., 2003). Similarly for CTS, Tecchio et al. demonstrated by MEG that the D1 to D5 cortical representation distance decreased in CTS patients when pain predominated, but increased with predominant paresthesias (Tecchio et al., 2002). The increase and decrease was specifically due to a shift in D5 and not in D1. Our CTS patient cohort experienced predominant paresthesias, and while the average D5 cortical representation was also more medial than for healthy adults (consistent with Tecchio et al.), this shift did not reach statistical significance. As we did not resolve the D1 representation, it is unclear whether this digit was shifted medially in CTS patients (as we found for D2) or was stationary (as found by Tecchio et al.). However, the improved spatial resolution of fMRI with surface based analysis tools (compared to MEG) allowed us to explore cortical somatotopy for adjacent CTS-affected digits (D2, D3), in addition to D5.

Limitations

While both groups were instructed identically in regard to attention, it is possible that activation differences between groups resulted from variability in attention applied to the stimulus during fMRI scanning, attention is a known modulator of somatosensory activation (Nelson et al., 2004), and CTS patients may be hypervigilant as a result of their symptoms, and hence more attentive to stimuli at their digits. However, other investigators have noted that attention modulation of somatosensory response is more pronounced in SII than in SI (Burton et al., 1999; Fujiwara et al., 2002). Furthermore, there was not a significant difference in fMRI signal over successive ON-blocks for either group—suggesting against time-variant attentional modulation (habituation).

Our somatotopy results demonstrated that CTS was associated with less separation between median nerve innervated D2 and D3, as compared to healthy adults (CTS: 3.8 ± 1.0 mm; Healthy: 7.5 ± 1.2 mm; $P < 0.05$). It can be argued that this surface-space difference is on the order of our imaging voxel size. However, statistically significant differences between groups at or below the sampling resolution can exist, and can be attributed to increased sensitivity due to inter-subject averaging and the use of center-of-mass (i.e., weighted average) calculations.

In summary, this study represents the first exploration of CTS by fMRI. The increased cortical activity and blurred digit representations noted for CTS patients may be the central cortical manifestation of patients' peripheral nerve dysfunction. Conversely, these central manifestations may themselves influence subsequent processing in other brain regions (e.g., cognitive, affective) and thereby influence patients' subjective evaluation of their pain and paresthesias. In fact, the role of paresthesias in cortical reorganization has been poorly studied and deserves more attention. Future studies should also evaluate CTS patients with predominant pain over paresthesias, as differences may exist between CTS groups depending on the predominant symptom. Finally, we hope to explore the potential for the use of fMRI as an objective and quantitative tool by which different therapies for CTS may be evaluated.

Acknowledgments

This research was supported by grants from the NIH: NCCAM (K01-AT002166-01, P01-AT002048-02, R21-AT001361-01), NCRR (P41RR14075), and the Mental Illness and Neuroscience

Discovery (MIND) Institute, as well as the Department of Physical Medicine and Rehabilitation Mini-grant Program, Harvard Medical School (#R02034). We would also like to acknowledge Dr. Judith D. Schaechter, who contributed to data analysis and provided feedback on a draft of the manuscript.

References

Allard, T., Clark, S.A., Jenkins, W.M., Merzenich, M.M., 1991. Reorganization of somatosensory area 3b representations in adult owl monkeys after digital syndactyly. J. Neurophysiol. 66, 1048–1058.

Blankenburg, F., Ruben, J., Meyer, R., Schwiemann, J., Villringer, A., 2003. Evidence for a rostral-to-caudal somatotopic organization in human primary somatosensory cortex with mirror-reversal in areas 3b and 1. Cereb. Cortex 13, 987–993.

Brown, T.H., Chapman, P.F., Kairiss, E.W., Keenan, C.L., 1988. Long-term synaptic potentiation. Science 242, 724–728.

Buonomano, D.V., Merzenich, M.M., 1998. Cortical plasticity: from synapses to maps. Annu. Rev. Neurosci. 21, 149–186.

Burton, H., Abend, N.S., MacLeod, A.M., Sinclair, R.J., Snyder, A.Z., Raichle, M.E., 1999. Tactile attention tasks enhance activation in somatosensory regions of parietal cortex: a positron emission tomography study. Cereb. Cortex 9, 662–674.

Calford, M.B., Tweedale, R., 1988. Immediate and chronic changes in responses of somatosensory cortex in adult flying-fox after digit amputation. Nature 332, 446–448.

Clark, S.A., Allard, T., Jenkins, W.M., Merzenich, M.M., 1988. Receptive fields in the body-surface map in adult cortex defined by temporally correlated inputs. Nature 332, 444–445.

Cox, R.W., 1996. AFNI: software for analysis and visualization of functional magnetic resonance neuroimages. Comput. Biomed. Res. 29, 162–173.

Dale, A.M., Fischl, B., Sereno, M.I., 1999. Cortical surface-based analysis: I. Segmentation and surface reconstruction. NeuroImage 9, 179–194.

Disbrow, E., Roberts, T., Krubitzer, L., 2000. Somatotopic organization of cortical fields in the lateral sulcus of Homo sapiens: evidence for SII and PV. J. Comp. Neurol. 418, 1–21.

Druschky, K., Kaltenhauser, M., Hummel, C., Druschky, A., Huk, W.J., Stefan, H., Neundorfer, B., 2000. Alteration of the somatosensory cortical map in peripheral mononeuropathy due to carpal tunnel syndrome. NeuroReport 11, 3925–3930.

Dykes, R.W., 1997. Mechanisms controlling neuronal plasticity in somatosensory cortex. Can. J. Physiol. Pharmacol. 75, 535–545.

Eisenberg, E., Chistyakov, A.V., Yudashkin, M., Kaplan, B., Hafner, H., Feinsod, M., 2005. Evidence for cortical hyperexcitability of the affected limb representation area in CRPS: a psychophysical and transcranial magnetic stimulation study. Pain 113, 99–105.

Fischl, B., Sereno, M.I., Dale, A.M., 1999a. Cortical surface-based analysis. II: Inflation, flattening, and a surface-based coordinate system. NeuroImage 9, 195–207.

Fischl, B., Sereno, M.I., Tootell, R.B., Dale, A.M., 1999b. High-resolution intersubject averaging and a coordinate system for the cortical surface. Hum. Brain Mapp. 8, 272–284.

Flor, H., Braun, C., Elbert, T., Birbaumer, N., 1997. Extensive reorganization of primary somatosensory cortex in chronic back pain patients. Neurosci. Lett. 224, 5–8.

Francis, S.T., Kelly, E.F., Bowtell, R., Dunseath, W.J., Folger, S.E., McGlone, F., 2000. fMRI of the responses to vibratory stimulation of digit tips. NeuroImage 11, 188–202.

Fujiwara, N., Imai, M., Nagamine, T., Mima, T., Oga, T., Takeshita, K., Toma, K., Shibasaki, H., 2002. Second somatosensory area (SII) plays a significant role in selective somatosensory attention. Brain Res. Cogn. Brain Res. 14, 389–397.

Gelnar, P.A., Krauss, B.R., Szeverenyi, N.M., Apkarian, A.V., 1998. Fingertip representation in the human somatosensory cortex: an fMRI study. NeuroImage 7, 261–283.

Genovese, C.R., Lazar, N.A., Nichols, T., 2002. Thresholding of statistical maps in functional neuroimaging using the false discovery rate. NeuroImage 15, 870–878.

Godde, B., Spengler, F., Dinse, H.R., 1996. Associative pairing of tactile stimulation induces somatosensory cortical reorganization in rats and humans. NeuroReport 8, 281–285.

Hebb, D., 1949. The Organization of Behavior. Wiley and Sons, New York.

Hodzic, A., Veit, R., Karim, A.A., Erb, M., Godde, B., 2004. Improvement and decline in tactile discrimination behavior after cortical plasticity induced by passive tactile coactivation. J. Neurosci. 24, 442–446.

Iwamura, Y., Tanaka, M., Sakamoto, M., Hikosaka, O. (Eds.), Comparison of the Hand and Finger Representation in Areas 3, 1, and 2 of the Monkey Somatosensory Cortex. Alan R. Liss, Inc., New York.

Jenkins, W.M., Merzenich, M.M., Ochs, M.T., Allard, T., Guic-Robles, E., 1990. Functional reorganization of primary somatosensory cortex in adult owl monkeys after behaviorally controlled tactile stimulation. J. Neurophysiol. 63, 82–104.

Jenkinson, M., Bannister, P., Brady, M., Smith, S., 2002. Improved optimization for the robust and accurate linear registration and motion correction of brain images. NeuroImage 17, 825–841.

Ji, R.R., Kohno, T., Moore, K.A., Woolf, C.J., 2003. Central sensitization and LTP: do pain and memory share similar mechanisms? Trends Neurosci. 26, 696–705.

Jones, E.G., 1993. GABAergic neurons and their role in cortical plasticity in primates. Cereb. Cortex 3, 361–372.

Juottonen, K., Gockel, M., Silen, T., Hurri, H., Hari, R., Forss, N., 2002. Altered central sensorimotor processing in patients with complex regional pain syndrome. Pain 98, 315–323.

Kaas, J.H., Nelson, R.J., Sur, M., Lin, C.S., Merzenich, M.M., 1979. Multiple representations of the body within the primary somatosensory cortex of primates. Science 204, 521–523.

Kurth, R., Villringer, K., Mackert, B.M., Schwiemann, J., Braun, J., Curio, G., Villringer, A., Wolf, K.J., 1998. fMRI assessment of somatotopy in human Brodmann area 3b by electrical finger stimulation. NeuroReport 9, 207–212.

Levine, D.W., Simmons, B.P., Koris, M.J., Daltroy, L.H., Hohl, G.G., Fossel, A.H., Katz, J.N., 1993. A self-administered questionnaire for the assessment of severity of symptoms and functional status in carpal tunnel syndrome. J. Bone Jt. Surg. Am. 75, 1585–1592.

Levy, L.M., Ziemann, U., Chen, R., Cohen, L.G., 2002. Rapid modulation of GABA in sensorimotor cortex induced by acute deafferentation. Ann. Neurol. 52, 755–761.

Ma, D., Liveson, J., 1983. Nerve Conduction Handbook. FA Davis Co., Philadelphia.

Maihofner, C., Handwerker, H.O., Neundorfer, B., Birklein, F., 2003. Patterns of cortical reorganization in complex regional pain syndrome. Neurology 61, 1707–1715.

Maldjian, J.A., Gottschalk, A., Patel, R.S., Detre, J.A., Alsop, D.C., 1999. The sensory somatotopic map of the human hand demonstrated at 4 Tesla. NeuroImage 10, 55–62.

McGlone, F., Kelly, E.F., Trulsson, M., Francis, S.T., Westling, G., Bowtell, R., 2002. Functional neuroimaging studies of human somatosensory cortex. Behav. Brain Res. 135, 147–158.

Merzenich, M.M., Kaas, J.H., Wall, J., Nelson, R.J., Sur, M., Felleman, D., 1983. Topographic reorganization of somatosensory cortical areas 3b and 1 in adult monkeys following restricted deafferentation. Neuroscience 8, 33–55.

Merzenich, M.M., Nelson, R.J., Stryker, M.P., Cynader, M.S., Schoppmann, A., Zook, J.M., 1984. Somatosensory cortical map changes following digit amputation in adult monkeys. J. Comp. Neurol. 224, 591–605.

Mima, T., Sadato, N., Yazawa, S., Hanakawa, T., Fukuyama, H., Yonekura, Y., Shibasaki, H., 1999. Brain structures related to active and passive finger movements in man. Brain 122 (Pt. 10), 1989–1997.

Mogyoros, I., Bostock, H., Burke, D., 2000. Mechanisms of paresthesias arising from healthy axons. Muscle Nerve 23, 310–320.

Moore, C.I., Stern, C.E., Corkin, S., Fischl, B., Gray, A.C., Rosen, B.R., Dale, A.M., 2000. Segregation of somatosensory activation in the human rolandic cortex using fMRI. J. Neurophysiol. 84, 558–569.

Naito, E., Roland, P.E., Ehrsson, H.H., 2002. I feel my hand moving: a new role of the primary motor cortex in somatic perception of limb movement. Neuron 36, 979–988.

Nelson, A.J., Staines, W.R., Graham, S.J., McIlroy, W.E., 2004. Activation in SI and SII: the influence of vibrotactile amplitude during passive and task-relevant stimulation. Brain Res. Cogn. Brain Res. 19, 174–184.

Nishimura, A., Ogura, T., Hase, H., Makinodan, A., Hojo, T., Katsumi, Y., Yagi, K., Mikami, Y., Kubo, T., 2003. Objective evaluation of sensory function in patients with carpal tunnel syndrome using the current perception threshold. J. Orthop. Sci. 8, 625–628.

Nora, D.B., Becker, J., Ehlers, J.A., Gomes, I., 2005. What symptoms are truly caused by median nerve compression in carpal tunnel syndrome? Clin. Neurophysiol. 116, 275–283.

Ochoa, J.L., Torebjork, H.E., 1980. Paraesthesiae from ectopic impulse generation in human sensory nerves. Brain 103, 835–853.

Overduin, S.A., Servos, P., 2004. Distributed digit somatotopy in primary somatosensory cortex. NeuroImage 23, 462–472.

Papanicolaou, G.D., McCabe, S.J., Firrell, J., 2001. The prevalence and characteristics of nerve compression symptoms in the general population. J. Hand Surg. [Am.] 26, 460–466.

Penfield, W., Boldrey, E., 1937. Somatic motor and sensory representation in the cerebral cortex of man as studied by electrical stimulation. Brain 60, 389–443.

Pilz, K., Veit, R., Braun, C., Godde, B., 2004. Effects of co-activation on cortical organization and discrimination performance. NeuroReport 15, 2669–2672.

Rademacher, J., Caviness Jr., V.S., Steinmetz, H., Galaburda, A.M., 1993. Topographical variation of the human primary cortices: implications for neuroimaging, brain mapping, and neurobiology. Cereb. Cortex 3, 313–329.

Rauschecker, J.P., 1991. Mechanisms of visual plasticity: Hebb synapses, NMDA receptors, and beyond. Physiol. Rev. 71, 587–615.

Rygh, L.J., Svendsen, F., Fiska, A., Haugan, F., Hole, K., Tjolsen, A., 2005. Long-term potentiation in spinal nociceptive systems—How acute pain may become chronic. Psychoneuroendocrinology 30, 959–964.

Schwenkreis, P., Janssen, F., Rommel, O., Pleger, B., Volker, B., Hosbach, I., Dertwinkel, R., Maier, C., Tegenthoff, M., 2003. Bilateral motor cortex disinhibition in complex regional pain syndrome (CRPS) type I of the hand. Neurology 61, 515–519.

Smith, S.M., 2002. Fast robust automated brain extraction. Hum. Brain Mapp. 17, 143–155.

Stevens, J.C., 1997. AAEM minimonograph #26, the electrodiagnosis of carpal tunnel syndrome. American Association of Electrodiagnostic Medicine. Muscle Nerve 20, 1477–1486.

Strick, P.L., Preston, J.B., 1978. Sorting of somatosensory afferent information in primate motor cortex. Brain Res. 156, 364–368.

Tecchio, F., Padua, L., Aprile, I., Rossini, P.M., 2002. Carpal tunnel syndrome modifies sensory hand cortical somatotopy: a MEG study. Hum. Brain Mapp. 17, 28–36.

Tinazzi, M., Zanette, G., Volpato, D., Testoni, R., Bonato, C., Manganotti, P., Miniussi, C., Fiaschi, A., 1998. Neurophysiological evidence of neuroplasticity at multiple levels of the somatosensory system in patients with carpal tunnel syndrome. Brain 121 (Pt. 9), 1785–1794.

Wang, X., Merzenich, M.M., Sameshima, K., Jenkins, W.M., 1995. Remodelling of hand representation in adult cortex determined by timing of tactile stimulation. Nature 378, 71–75.

White, L.E., Andrews, T.J., Hulette, C., Richards, A., Groelle, M., Paydarfar, J., Purves, D., 1997. Structure of the human sensorimotor system. II: Lateral symmetry. Cereb. Cortex 7, 31–47.

Wong, Y.C., Kwan, H.C., MacKay, W.A., Murphy, J.T., 1978. Spatial organization of precentral cortex in awake primates: I. Somatosensory inputs. J. Neurophysiol. 41, 1107–1119.

Woolrich, M.W., Ripley, B.D., Brady, M., Smith, S.M., 2001. Temporal autocorrelation in univariate linear modeling of fMRI data. NeuroImage 14, 1370–1386.

Woolsey, C.N., Erickson, T.C., Gilson, W.E., 1979. Localization in somatic sensory and motor areas of human cerebral cortex as determined by direct recording of evoked potentials and electrical stimulation. J. Neurosurg. 51, 476–506.

You, H., Simmons, Z., Freivalds, A., Kothari, M.J., Naidu, S.H., 1999. Relationships between clinical symptom severity scales and nerve conduction measures in carpal tunnel syndrome. Muscle Nerve 22, 497–501.

Yousry, T.A., Schmid, U.D., Alkadhi, H., Schmidt, D., Peraud, A., Buettner, A., Winkler, P., 1997. Localization of the motor hand area to a knob on the precentral gyrus. A new landmark. Brain 120 (Pt. 1), 141–157.